ELSEVIER

Nuclear Instruments and Methods in Physics Research A 401 (1997) 144–155

NUCLEAR INSTRUMENTS & METHODS IN PHYSICS RESEARCH Section A

Measurement and control of the ^{214}Bi contamination in the ββ NEMO-2 experiment

NEMO Collaboration

R. Arnold[a], C. Augier[b], A. Barabash[c], D. Blum[b], V. Brudanin[d], J.E. Campagne[b], D. Dassié[e], V. Egorov[d], R. Eschbach[e], J.L. Guyonnet[a], F. Hubert[e], Ph. Hubert[e], S. Jullian[b], I. Kisel[d], O. Kochetov[d], V.N. Kornoukov[c], V. Kovalenko[d], D. Lalanne[b], F. Laplanche[b], F. Leccia[e], I. Linck[a], C. Longuemare[f,*], F. Mauger[f], P. Mennrath[e], H.W. Nicholson[g], A. Nozdrin[d], F. Piquemal[e], O. Purtov[h], J.-L. Reyss[i], F. Scheibling[a], J. Suhonen[j], C.S. Sutton[g], G. Szklarz[b], V.I. Tretyak[h], V. Umatov[c], I. Vanushin[c], A. Vareille[e], Yu. Vasilyev[h], Ts. Vylov[d], V. Zerkin[h]

[a] *IReS, IN2P3-CNRS et Université Louis Pasteur, 67037 Strasbourg, France*
[b] *LAL, IN2P3-CNRS et Université Paris-Sud, 91405 Orsay, France*
[c] *ITEP, Moscow, Russia*
[d] *JINR, Dubna, Russia*
[e] *CENBG, IN2P3-CNRS et Université de Bordeaux, 33170 Gradignan, France*
[f] *LPC-ISMRA, IN2P3-CNRS et Université de Caen, 14050 Caen Cedex, France*
[g] *MHC, South Hadley, Massachusetts 01075, USA*
[h] *INR, Kiev, Ukraine*
[i] *CFR, CNRS, 91190 Gif sur Yvette, France*
[j] *JYVÄSKYLÄ University, 40351 Jyväskylä, Finland*

Received 19 February 1997; received in revised form 23 July 1997

Abstract

In the double beta decay (ββ) experiment NEMO-2, the ^{214}Bi radioactivity has been measured as background for the ββ processes. The analysis of the ^{214}Bi contamination has been performed via the signature of ^{214}Po alpha decay. This method has been applied to data taken with enriched ^{100}Mo and ^{116}Cd sources. At the level of NEMO-2's sensitivity, in a 1.0 mole yr study of enriched material, the contamination of the sources can be measured in the range of 2.0 mBq kg^{-1}. The effects of deposited contamination by ^{222}Rn are also discussed and estimated at the level of 0.3 mBq per square meter of source foil. Backgrounds for neutrinoless double beta decay (ββ0ν) are deduced from these measurements and the consequences for the higher sensitivity ββ experiment NEMO-3 are drawn.

* Corresponding author. Tel.: +33 2 31 45 25 15; fax: +33 2 31 45 25 49; e-mail: longuemare@caelav.in2p3.fr.

PII S0168-9002(97)01013-9

1. Introduction

Neutrinoless double beta ($\beta\beta0\nu$) decay which violates the lepton number conservation law is an important probe to physics beyond the standard model [1]. During the last decade, new high sensitivity experiments have pushed the limits of neutrinoless double beta decay lifetime into the range of 10^{24-25} years for ^{76}Ge experiments [2].

The NEMO experiment is an international collaboration which aims to study the $\beta\beta0\nu$ lifetime of ^{100}Mo and other nuclei in the range of 10^{25} years. This goal will be reached with a large detector named NEMO-3 installed in the Fréjus underground laboratory (LSM[1])near Modane at the French–Italian border. The double beta decay detector NEMO-3 will be a third generation detector following NEMO-1 and NEMO-2 and will be the final step of a research and development program initiated in 1989 to design an experiment probing the neutrino mass in the range of a fraction of an eV for ^{100}Mo and for various other nuclei [3]. This detector is designed to accommodate an enriched ^{100}Mo source of 10 kg with extremely low radioactivity levels and to run for several years.

To achieve such high sensitivity $\beta\beta$ experiments, it is crucial to understand and to reduce the backgrounds especially in the highest part of the $\beta\beta$ energy spectrum. One of the problems in such experiments is the need for very low levels of ^{214}Bi radioactivity. The ^{214}Bi isotope is a source of background which is part of the ^{238}U decay chain and is present in trace amounts in many materials. Its beta decay followed by gamma conversion produces electron pairs with a summed energy spectrum up to 3.27 MeV. The radioactive ^{222}Rn gas has to be considered in this analysis because the ^{214}Bi isotope is a downstream member of radon chain and radon has a well known capability to diffuse and to transport radioactivity. The $\beta\beta2\nu$ signals of ^{100}Mo and ^{116}Cd have been analyzed with NEMO-2 [4,5]. Since these signals were significant, the ^{214}Bi background was negligible for those measurements but the ^{214}Bi backgrounds have to be very low for studies of the $\beta\beta0\nu$ processes at the level of sensitivity of NEMO-3.

In this paper, the background due to ^{214}Bi is analysed using the data taken with NEMO-2. This prototype detector is shown in Fig. 1. It is built as a modular cubic drift chamber filled with helium–alcohol gas, surrounding a thin one square meter source foil of $\beta\beta$ emitter which divides the chamber in two parts. The cube is closed on two opposite sides by scintillator walls. An iron and lead shielding surrounds the detector which is located in the LSM laboratory. The source weighs a few hundred grams; its thickness is only 40 μm in order to let the $\beta\beta$ electrons leave the foil so as to be detected in the tracking chamber and measured by the scintillators. This detector and its performance have been described elsewhere [4–6]. The expected signal of $\beta\beta0\nu$ decays is characterized by two electron tracks originating from the foil with the maximum energy $Q_{\beta\beta}$. The detection efficiency for such events is about 4% for ^{100}Mo ($Q_{\beta\beta} = 3.034$ MeV).

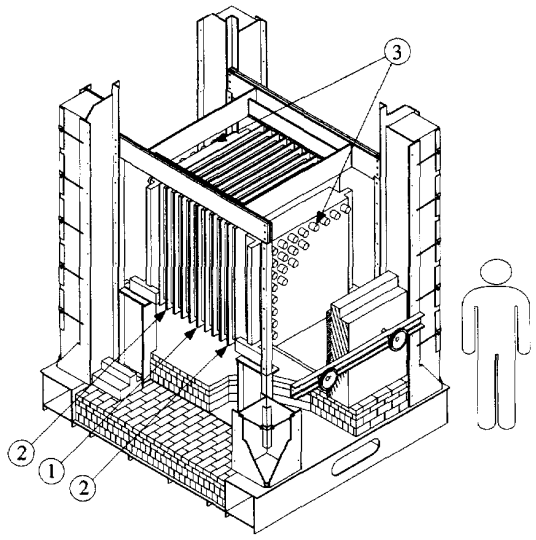

Fig. 1. The NEMO-2 detector without shielding: 1 – Central frame supporting the source. 2 – Copper frames which support the Geiger cells. 3 – 8 × 8 arrays of scintillator counters for phase 3, then 5 × 5 for phases 4 and 5.

The means for studying the ^{214}Bi contamination are through germanium gamma spectroscopy and recorded events of NEMO-2. More specifically, the events of interest are the electron-gamma events in the higher part of the energy spectrum ($E_\gamma > 1.0$ MeV, $E_\gamma + E_e > 1.5$ MeV [6]) or electron–gamma–alpha events with a signature of the ^{214}Bi–^{214}Po–^{210}Pb

[1] Laboratoire Souterrain de Modane.

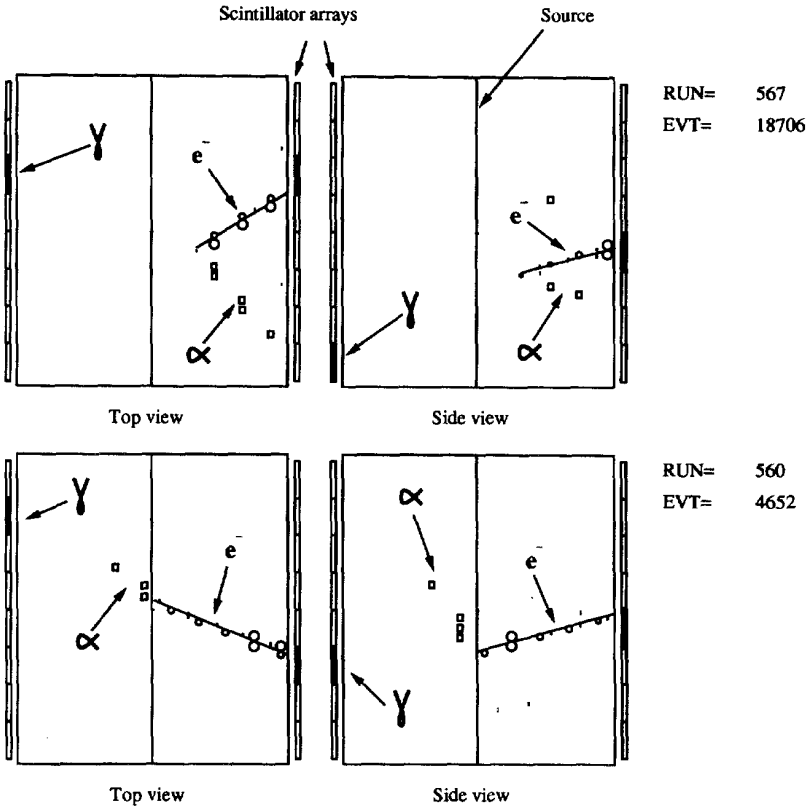

Fig. 2. Projected view of (α) events recorded in NEMO-2. The circles and small bars represent the transverse and longitudinal hits of the prompt event and identify an electron track (e^-) in the Geiger tracking chamber. The radius of circles is the drift distance with respect to the anode wire. The Geiger delayed hits are represented by squares ("Top view" with (X–Z) position, "Side view" with (Y–Z) position) and are identified as alpha particles (α). A hit scintillator block (black rectangle) corresponds to a gamma ray (γ) when it is not associated with an electron track.

cascade. We present here results obtained by the last method which was previously studied by others [7,8]. The signature of the ^{214}Bi beta decay is obtained from its daughter nucleus ^{214}Po which is an alpha emitter with a lifetime of $T_{1/2} = 164\,\mu s$ [9]. Alpha particles from ^{214}Po are detected as short delayed tracks in the drift chamber; the maximum range in the gas of NEMO-2 at atmospheric pressure[2] is 32 cm. The NEMO-2 detector as well as the future NEMO-3 detector is equipped with drift chamber electronics able to record all delayed hits during one millisecond after the trigger. Position and delay time are recorded for each hit thus allowing the study of correlations in space and time. In NEMO-2, the measurement of delayed hit time is done with a resolution of 4 μs. The three-dimensional track reconstruction is made by cross-checking the two-dimensional measurements from both projected views; a couple of *alpha* events are presented in Fig. 2.

2. Data taking with NEMO-2

Data samples used in this analysis were taken at different times under different physical conditions

[2] The average atmospheric pressure in the LSM laboratory is 880 hPa.

referenced as phases 3, 4 and 5. These changes of the experimental environment gave us opportunities to focus the study on peculiar aspects of radon and ^{214}Bi contamination. Working at the limit of sensitivity of the detector, we used the different samples in a discriminating manner to show several effects of the contamination.

Total exposure for phase 3 was 4941 h with high purity enriched and natural molybdenum foils and with standard photomultiplier tubes (PMT). The basic trigger during this phase required two scintillators to fire within a 50 ns coincidence time, plus a track made of at least 4 cells in the same side of the chamber. The PMT threshold was set at 50 keV. We observed a trigger rate of about 0.2 Hz. The data were submitted to a filter based mainly on time-of-flight cuts in order to reject external events originating far from the foil. The rejection factor was about 97%. The phase 3 run corresponds to the first measurement of ^{100}Mo $\beta\beta2\nu$ decay with the NEMO-2 detector. During this phase, the ventilation in the underground laboratory failed to work continuously for about three weeks. As a consequence, we observed an increase of radon gas in the atmosphere of the laboratory from a mean value of 25 Bq m^{-3} up to 100 Bq m^{-3}. At the end of this 500 h period, the radon contamination decreased to its initial value. We used this period to discriminate the effects due to the external radon gas; it was possible to show a correlation between the *alpha* event rate and the radon contamination of the atmosphere. As it will be presented, this leads us to identify the contribution of radon in NEMO-2 data.

Phase 4 was a test run of only 2259 h using the same molybdenum foil as in phase 3 but with bigger scintillators and low radioactivity photomultiplier tubes. NEMO-2 ran with a trigger requiring only one PMT plus a track (at least 4 hit Geiger cells). A better detection efficiency for gamma rays was obtained with the thicker scintillation blocks. No filter was applied on the data, giving a larger sample with event vertices which are located far from the source foil in the tracking chamber. The external radon contamination was stable and low during the phase 4 and it was thus not possible to discriminate the radon effects by the means of a correlation with external radon activity. Instead, the vertex position of the selected events was studied, and it was concluded that radon was deposited on the inner surfaces of the tracking chamber.

Phase 5 was a 6633 h run with a high purity cadmium source and no other changes to the apparatus. We used the length of the α track to estimate the amount of radon deposited and internal ^{214}Bi contamination in the $\beta\beta$ source. The analysis in phase 5 reaches its limit of sensitivity because the sample of *alpha* events, when selected with the same criteria used in previous phases, was left with a rather large background of spurious random events.

During the phases 4 and 5 with the low radioactive PMT's, the largest fraction of trigger events[3] was due to the radioactivity in the detector itself which induces Compton scattering in the foil or in the scintillator blocks. Nevertheless the observed variations of the trigger rate have been correlated with the radon activity (^{222}Rn) in the atmosphere of the LSM [6]. At the concentration of 20 Bq m^{-3}, the radon decay chain explains 10% (21%) of the raw trigger rate in phase 3 (phases 4 and 5). The experimental variation of the trigger rate has been explained quantitatively by the simulation of the radon activity of the small amount of air approaching the detector through the shielding. Experimental running conditions are summarized in Table 1.

3. Selection

The ^{214}Bi isotope has a lifetime of 19.7 mn; it is continuously regenerated by the ^{238}U–^{222}Rn chain. The total energy release in the decay is 3.27 MeV. Considering the decay scheme of ^{214}Bi, the NEMO-2 apparatus can distinguish three inclusive decay channels: one electron without gamma ray, one electron with gamma rays and two electrons with gamma rays; from nuclear data tables, the branching ratios are respectively 18%, 80% and 2% [9]. The resulting ^{214}Po final nucleus undergoes an alpha decay with a half-life of 164 μs. The selection of events with a delayed alpha track in the NEMO-2 detector has been done within a two step process. First, events with a *cluster* of delayed hits have been searched for by program and then a visual scanning of the events was necessary to achieve the selection of the sample. The backgrounds in this sample come from radioactivity and from additional

[3] (1e), (2e), (1e, nγ) events.

Table 1
Data collection: "Track" stands for "at least 4 hit Geiger cells in the tracking chamber"

Phase (source)	Time (h)	Mass (g)	Trigger conditions	Mean trigger rate (Hz)	^{214}Bi cont. of source[a] (mBq kg^{-1})
3 ($^{100+nat.}$Mo)	4941	172 + 163	≥2 PMT +Track	0.23	<20
4 ($^{100+nat.}$Mo)	2259	172 + 163	≥1 PMT +Track	0.45	<20
5 ($^{116+nat.}$Cd)	6633	152 + 143	≥1 PMT +Track	0.48	<5

[a] From preliminary gamma-ray spectrometry measurements of source materials.

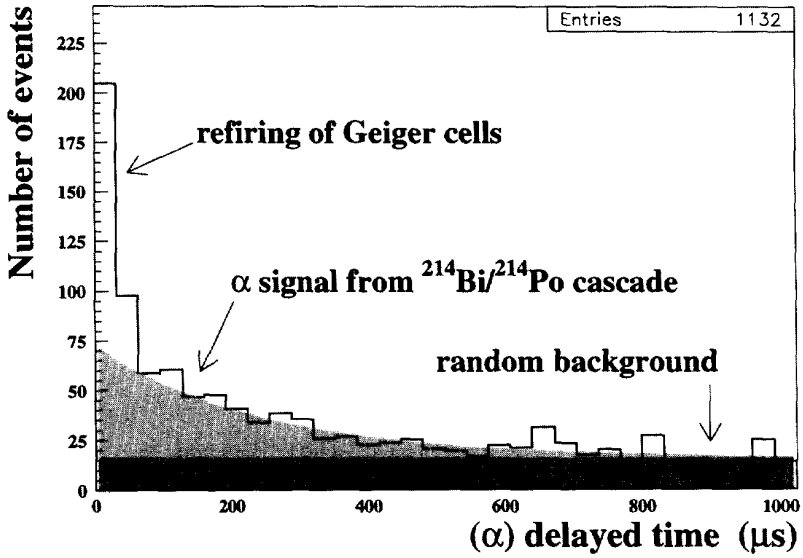

Fig. 3. Delayed time distribution from the preselected sample (1132 events) for phase 3 (4941 h of data collection, 1 bin ≡ 32 μs).

and spurious hits called *refiring* cells which are due to the local instability of the Geiger plasma.

3.1. Automatic preselection

A cluster has been defined by the following criteria: to reject refiring, a hit is only considered if its delay is over 20 μs (Geiger propagation time). A cluster is a group of more than 3 hits and less than 12 hits within 16 μs; they have to be located in the same side of the tracking chamber with respect to the source, regardless of the projected views. Events with one cluster are considered. The time of the cluster is averaged over the hits. These criteria have been defined taking into account the properties of alpha tracks and the granularity of the Geiger chamber.

The time distribution of the selected events is presented in Fig. 3 for phase 3. The signal of ^{214}Po hardly appears in this distribution for which the exponential shape of the distribution (light gray) is in the 100–500 μs range and is hidden with a rather large random background (dark gray) and with clusters due to refiring at small delay time (peak in bins 1–2). This result led us to display the prompt and delayed hits on

Table 2
Selection steps in phases 3, 4 and 5

Phase	Number of used events	Preselection of *clusters*	Final (α) sample
3	$1.44\,10^5$ [a]	1132	326
4	$2.71\,10^5$ [a]	5719	783
5	$11.50\,10^6$	25866 [b]	3339/348 [c]

[a] >1 PMT events.
[b] 1 PMT events with their vertex on the foil.
[c] Sample with additional cuts (see Section 4.2).

a graphics terminal in order to perform a second stage selection through visual scanning.

3.2. Visual scanning

The aim for the scanning was to control the selected clusters as a track in the chamber with the typical features of an alpha particle. The cluster must be correlated in space with the prompt event responsible for the trigger. We require the cluster to form a line of at least 3 hits (considering both projected views) and intercepting a possible vertex on a prompt electron track. Only one missing hit along the track is allowed. The identified vertex is taken as the event vertex. The visually selected delayed track is measured as a straight track in both views. In order to reject ambiguous events found at the border of the detector, a fiducial cut is applied: the vertex has to be 6 cm away from the copper walls of the tracking chamber and 10 cm away from the scintillators. Events in the final sample are called *alpha* events. The efficiency of scanning has been tested by double scanning; it is better than 95%. Table 2 summarizes the selection steps and shows the corresponding statistics in phases 3–5.

The time distribution of the 326 event sample for phase 3 is displayed in Fig. 4 (solid line). Its characteristics, exponential shape and slope are compatible with the expected period of 164 μs, and indicate that a ^{214}Bi/^{214}Po contamination exists inside NEMO-2. We detected 115 (α) events with their vertex on the foil ($|Z| < 3$ cm), and 211 with their vertex in the tracking chamber.

4. Analysis

From the fit of phase 3 data (Fig. 4), the contributions to the signal of (α) events are given in Table 3. The signal-to-background ratio value for the final sample is about 10 which provides a check on the scanning criteria.

4.1. Monte Carlo

The analysis of the topologies of the selected (α) sample is in agreement with the predictions of the Monte Carlo simulation used in the experiment. A typical (α) event is characterized by a delayed track following a prompt event consisting of electron tracks and gamma rays. The standard reconstruction of electron tracks and gamma rays uses the following criteria:

- an electron is defined as a well fitted track emerging from the foil, crossing one half of the tracking chamber and hitting a scintillator block (Fig. 2, bottom event); tracks with a large scattering angle are excluded and the energy deposited in the calorimeter must be greater than 200 keV;
- a gamma ray is defined by a cluster of hit scintillator blocks which are not associated with a track; the total energy deposited in the cluster must be greater than 200 keV;
- the maximum time difference between the two hit PMT's must be less than 2 ns: this time-of-flight cut is applied to reject events with their origin located outside the NEMO-2 detector;

The simulation of the detector is based on the CERN GEANT program. The Monte Carlo calculations take into account all decays of ^{214}Bi [9] and the propagation and interaction of the low energy electrons and gammas. The Monte Carlo has been used to analyse many decay channels for NEMO-2. We performed simulation runs of ^{214}Bi and ^{214}Po decays in and on the source foil, using the phase 3 conditions, to predict the (α) event topologies. Table 4 gives a comparison of the $(1e, \alpha, X)$,[4] $(2e, \alpha)$ and $(1e, 1\gamma, \alpha)$ topologies as found in the experimental sample and predicted

[4] X stands for other particles; then $(2e, \alpha)$ and $(1e, 1\gamma, \alpha)$ channels are subsets of the $(1e, \alpha, X)$ channel.

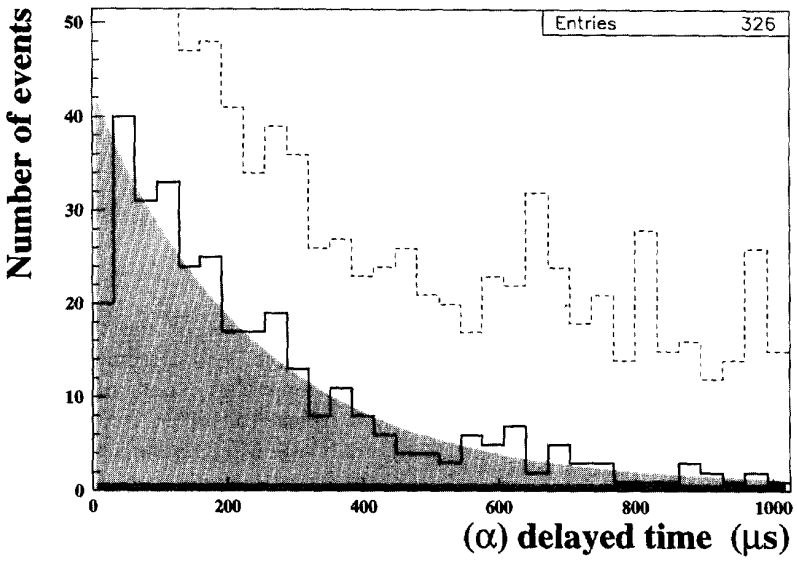

Fig. 4. Delayed time distribution from the final selected sample (solid line, 326 events) for phase 3 (4941 h of data collection). The small population in the first bin is due to the 20 μs cut at preselection (1 bin ≡ 32 μs). By comparison, the time distribution from the preselected sample is also shown (dashed, see Fig. 3).

Table 3
Contributions to the preselected and final (α) selected samples in phase 3 (respectively 1132 and 326 events). The values are given by the fit of the time distributions in Figs. 3 and 4

Contribution	Number of events (preselected sample)	Number of events (final sample)
^{214}Po signal	400 ± 48	297 ± 20
Random background	520 ± 38	21 ± 17
Refiring background	~ 210	~ 0
Signal-to-background ratio	~ 0.5	~ 10

Table 4
Classification of simulated and experimental (α) events in the topologies used in data analysis. The simulation generated 10^6 ^{214}Bi decays on the source

Channel	Simulated events	Experimental events (phase 3)	Expected sample from simulation[a]
(1e, α, X)	3560	115	115
(1e, 1γ, α)	1436	37	46 ± 6
(2e, α)	167	4	5 ± 1

[a] normalized to 115 events.

by the Monte Carlo program. Expected values in the last row are normalized to the experimental 115 event sample. The simulated characteristics are in agreement with the experimental ones. We checked that the relative rates of the various topologies are insensitive to the location of the contamination (internal or deposited), but the (α) detection efficiency is obviously strongly dependent on this location (see Table 5 in Section 4.3).

4.2. Radon effects in NEMO-2

We expect some internal contamination of the foil because of traces of ^{238}U. We also foresee some contamination coming from outside and transported by radon; the gas comes from LSM walls into the atmosphere of the experimental area. From there, it can reach the detector and enter it. This background can only be studied from the data recorded by the detector itself. It depends on the actual conditions in the

Table 5
Detection efficiencies of (α) events. Efficiencies account for different conditions in phases 3 and 5

Phase	Internal (10^{-3})	Deposited (10^{-3})
3	1.05 ± 0.05	3.65 ± 0.10
5	8.8 ± 0.6	18.6 ± 0.6

underground laboratory during the experiment, on the practical design of the detector and on the gas circulation in and around the detector. With NEMO-2, it is likely that radon gas can enter into the tracking chamber through the 36 μm thick mylar walls located in front of the scintillator walls and then can induce some contamination on the source foil.

The first evidence for external contamination by ^{222}Rn can be shown by correlating the (α) event rate with the ^{222}Rn activity in the laboratory. The measurement of the radon in the atmosphere is done every two hours by means of a commercial detector; the activity ranges between 10 and 100 Bq m^{-3} depending on the ventilation of the laboratory, the average value being 34 Bq m^{-3} during phase 3. The correlation of the (α) event rate with the radon rate is shown in Fig. 5 for phase 3. Data in Fig. 5 have been linearly extrapolated to 0 Bq m^{-3} ^{222}Rn activity. The extrapolated value has been interpreted as the ^{214}Bi internal contamination of the molybdenum source.

In order to measure the ^{222}Rn effect inside NEMO-2, we studied the distribution in space of the selected (α) events as shown in Fig. 6 for phase 4. We used phase 4 because the sample was unbiased with respect to the peripheral events which were rejected by the off-line filter in phase 3. The distribution shows two components in the sample: the first one (554 events) is randomly distributed in the chamber volume and the other (229 events, $|Z| < 3$ cm) is located on the foil at $Z = 0$. Events in the volume cannot be explained by the internal ^{214}Bi contamination of the wires which has been measured by gamma spectroscopy (< 33 mBq kg^{-1}) and can account for a maximum 25% of the sample at 90% CL. Consequently, we are left with the hypothesis that radon descendants are deposited on the nickel wires. The total surface of the wires in the tracking chamber is about 2 m^2 which is comparable with the surface of the source foil and the chamber inner walls.

Another test can be performed using the length of the delayed alpha tracks. For ^{214}Bi deposited on the foil, the alpha from ^{214}Po decay is mono-energetic and isotropic in distribution. On the contrary, for ^{214}Bi inside the foil, the alpha is likely to emerge close to the Z direction with a smaller range in the gas. Fig. 7 shows the range distributions of simulated alpha particles from ^{214}Bi contamination located respectively on the surface and in the source.

In phase 5, the event sample coming from the visual scanning is 3339 events. In this sample, the fit of the delayed time distribution gives an estimate of the signal-to-background ratio of about 1. The point is that the initial sample used in phase 5 is about one hundred times larger than the one used in phase 3 (Table 2), increasing the probability of random events. Then, the analysed sample has been restricted to events with their range between 6 and 40 cm, the delayed time lower than 700 μs, the energy collected by the hit PMT larger than 500 keV and $|\cos(\theta)| > 0.5$ (here θ is the angle between the alpha track and the Z detector axis). These cuts have been applied to reject background events due to low energy electrons emerging from the foil and randomly associated with a trigger. As a consequence, the (α) channel detection efficiency is reduced by a factor 4 leading to a final sample of 348 events but with a signal-to-background ratio increased to 6. The α range distribution of this sample is displayed in Fig. 8: the peak at 32 cm confirms a surface contamination. We conclude that radon induces some ^{214}Bi contamination on the source foil. From a fit of the range distribution, internal and external ^{214}Bi contaminations have been estimated. The results are presented in Section 4.3.

The origin of this radon contamination is likely the diffusion of external radon. In the case of a steady state, the Fick formula [10] provides a linear relation between the outside and inside activities which depends essentially on the diffusion constant D of radon through mylar. Defining $C_{\text{ext.}}$ as the radon activity in the atmosphere of the laboratory and $C_{\text{int.}}$ as the radon activity inside the detector, it gives:

$$C_{\text{int.}} = \frac{DS\tau}{eV} \times C_{\text{ext.}}$$

where $D = 8.4 \times 10^{-10}$ cm^2 s^{-1} at a temperature of 300 K [10]; S and e are the surface area and thickness of mylar windows, respectively, 1.88 m^2 and 36 μm;

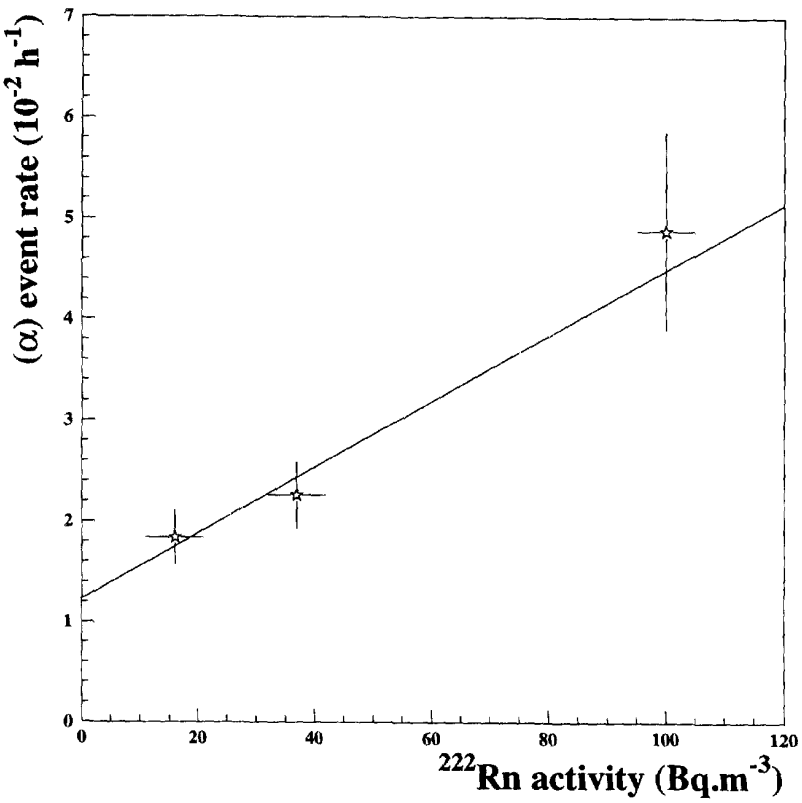

Fig. 5. Correlation of the (α) event rate with the ^{222}Rn activity in the laboratory (326 events, phase 3).

V is the volume of the chamber and equals 0.9 m^3; τ is the lifetime of radon in the chamber for which we take into account the gas ventilation in the tracking volume (the gas flow is about 20 $l\,h^{-1}$) and the radon radioactive life-time ($T_{1/2} = 3.82$ days) leading to $\tau = 32$ h. Using the average activity $C_{ext.} = 34$ Bq m^{-3} for phase 3, we expect $C_{int.}$ about 20 mBq m^{-3} which is comparable with 25 ± 10 mBq m^{-3} extracted from the (α) event rate detected in the chamber (in the realistic hypotheses of a uniform deposit on copper walls, source and wires and an average detection efficiency: 5×10^{-4}).

4.3. *Efficiencies, activities and* ββ0ν *background*

In order to get absolute values of activities in and on the foil, we have studied the efficiencies by Monte Carlo. The detection and recognition efficiencies of the present analysis are presented in Table 5 for ^{214}Bi located in the foil and on the foil.

The ^{214}Bi activities of the sources have been estimated using the most significant experimental information as described previously in this section. The correlation of the (α) event rate with the ^{222}Rn activity in the laboratory was used for phase 3 (Fig. 5), as well as the (α) range distribution for phase 5 (Fig. 8). The results are summarized in Table 6. The efficiencies have been taken from the simulation and the errors include statistics and estimated systematics.

From the measured contamination of the sources used in NEMO-2, we can estimate by simulation the ^{214}Bi background in the ββ0ν two electron channel selection [4,5]. At the level of sensitivity of NEMO-2, this background is negligible: as an example, in the conditions of phase 3 with ^{100}Mo, we expect a ^{214}Bi

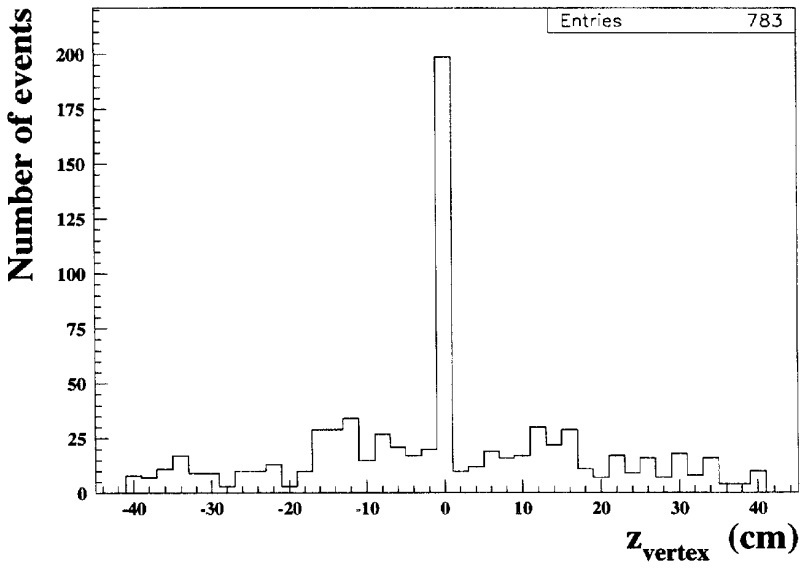

Fig. 6. Vertex distribution of the selected (α) events for phase 4. The Z coordinate is measured along the axis of the detector. $Z = 0$ is the foil position and $Z = \pm 50$ is the position of the scintillator walls.

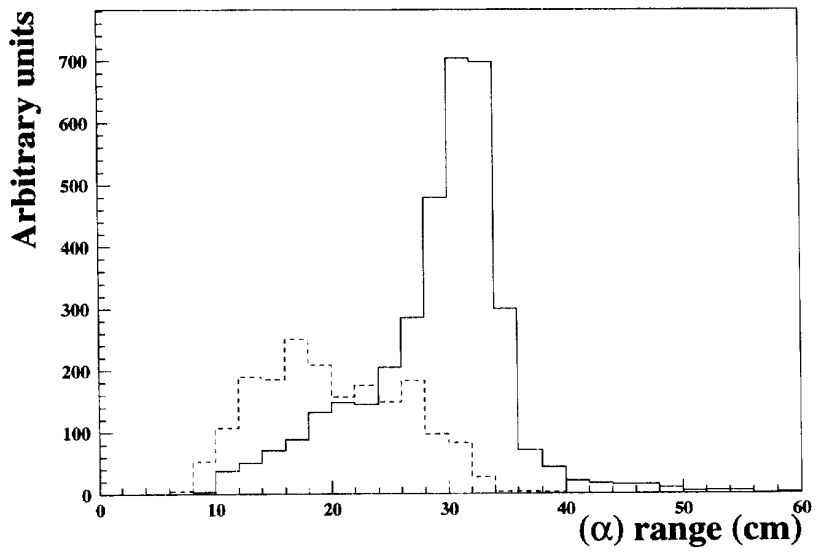

Fig. 7. Solid line: simulated α particle range distribution in the case of a ^{214}Bi superficial contamination of the foil. Dashed line: simulated α particle range distribution in the case of a ^{214}Bi internal contamination of the foil.

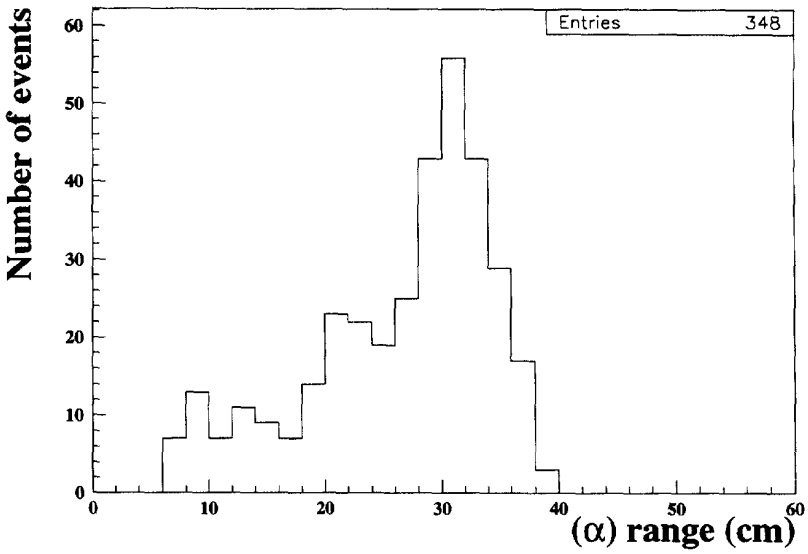

Fig. 8. Measured α particle range distribution for phase 5.

Table 6
Internal and deposited ^{214}Bi activities of the sources from (α) measurements

Phase (source)	Internal (mBq kg^{-1})	Deposited (mBq m^{-2})
3 ($^{100+nat.}$Mo)	10.0 ± 5.0	0.5 ± 0.3
5 ($^{116+nat.}$Cd)	1.6 ± 1.0	0.28 ± 0.07

background of 0.6 ± 0.3 events, 0.5 of which comes from the internal ^{214}Bi contamination of the source. At the level of sensitivity of NEMO-3, 50 kg yr of enriched ββ emitter with a ten times higher efficiency, it is clear that both internal and deposited ^{214}Bi contaminations have to be reduced by one order of magnitude [3].

5. Conclusion

We have obtained an estimation of the ^{214}Bi contamination of the molybdenum and cadmium foils used in NEMO-2. For the internal contamination, the result is compatible or better than other measurements obtained in collaboration with gamma spectroscopy. The level of 2 mBq kg^{-1} has typically been reached after a six month measurement. At this level, it has been shown that the radon gas diffusing from the rocks can penetrate the NEMO-2 detector and induce a significant part of the ^{214}Bi contamination of the source. The effect of radon deposit has been estimated and the results for both foils (Mo and Cd) are compatible. The (α) channel analysis is the only way to identify and to measure this background contribution which depends essentially on the running conditions.

We have extrapolated these measurements to interpret the few (2e) events detected in the 3 MeV region. The internal and deposited ^{214}Bi backgrounds contribute at about the same magnitude (i.e. a fraction of event per year), the deposited part being the smallest in the conditions of phases 3 and 5. ^{214}Bi contaminations, as measured, introduce no significant contribution to the ββ2ν signal analyses as mentioned in the NEMO-2 published papers [4,5].

The future NEMO-3 detector will be equipped with delayed alpha detection electronics. This should allow an efficient control of the ^{214}Bi internal contamination with an expected sensitivity of 0.1 mBq kg^{-1} in one year of measurement. The air-tightness of the NEMO-3 detector should suppress the diffusion of radon gas inside the tracking chamber.

Acknowledgements

We wish to thank the staff at the Fréjus Underground Laboratory for their technical support.

References

[1] H. Primakoff, S.P. Rosen, Ann. Rev. Nucl. Particle Sci. 31 (1981) 145.
[2] M. Günther et al., Phys. Rev. D 55 (1997) 54.
[3] D. Dassié et al., NEMO-3 Proposal, preprint LAL 94-29, 1994.
[4] D. Dassié et al., Phys. Rev. D 51 (1995) 2090.
[5] R. Arnold et al., Z. Phys. C 72 (1996) 239.
[6] R. Arnold et al., Nucl. Instr. and Meth. A 354 (1995) 338.
[7] M.K. Moe et al., Phys. Rev. C 22 (1980) 2186.
[8] M. Alston-Garnjost et al., Phys. Rev. Lett. 63 (1989) 1671.
[9] C.M. Lederer, V.S. Shirley (Eds.), Tables of Isotopes, Wiley-Interscience, 1978.
[10] J. Giridhar et al., Health Phys. 42 (1982) 723.